Structure and Mechanical Properties of Cellulose Derivatives/Soy Protein Isolate Blends

Ziyan Zhou,[1] Hua Zheng,[1] Ming Wei,[1] Jin Huang,[1,2] Yun Chen[3]

[1]*College of Chemical Engineering, Wuhan University of Technology, Wuhan 430070, China*
[2]*State Key Laboratory of Pulp and Paper Engineering, South China University of Technology, Guangzhou 510640, China*
[3]*Research Center for Medicine and Structural Biology, School of Medicine, Wuhan University, Wuhan 430072, China*

Received 19 January 2007; accepted 5 September 2007
DOI 10.1002/app.27323
Published online 27 November 2007 in Wiley InterScience (www.interscience.wiley.com).

ABSTRACT: Biodegradable and biocompatible composites based on soy protein isolate (SPI) and various cellulose derivatives have been prepared, and the dependence of structures and mechanical properties on the content and species of cellulose derivatives for the composites were investigated by X-ray diffraction, differential scanning calorimetry, scanning electron microscope, and tensile test. The selected cellulose derivatives, such as methyl cellulose (MC), hydroxyethyl cellulose (HEC), and hydroxypropyl cellulose, were miscible with SPI when the content of cellulose derivatives was low, and then the isolated crystalline domains, shown as the structures of network and great aggregate, formed with an increase of cellulose derivative content. The miscible blends could produce the higher strength, and even result in the simultaneous enhancement of strength and elongation for the HEC/SPI and MC/SPI blends. Meanwhile, the moderate content of great MC domains also reinforced the materials. However, the damage of original ordered structure in SPI gave the decreased modulus. Since all the components, i.e., cellulose derivatives and soy protein, are biocompatible, the resultant composites are not only used as environment-friendly material, but the biomedical application can be expected, especially for the tissue engineering scaffold. © 2007 Wiley Periodicals, Inc. J Appl Polym Sci 107: 3267–3274, 2008

Key words: soy protein; cellulose derivatives; blends; mechanical properties; structure-properties relationships

INTRODUCTION

The market of petroleum-based plastic will gradually be limited in applications because of its inevitable increase in price and pollution caused by nondegradability in the future.[1,2] As a result, biodegradable materials have attracted much attention for sustainable development and environmental conservation.[3,4] Furthermore, the extensive studies have been made for exploring potential use of polymeric materials derived from renewable resources.[3,5] Polysaccharides and proteins are the most abundant and important biomacromolecules in nature, which have been considered as the ideal substances of developing biodegradable materials. Considering that the combination of polysaccharides and proteins can express many biological functions and constitute the tissues of plants and animals, the composites based on biocompatible polysaccharides and proteins show a potential as biomedical materials.

Cellulose is the most abundant renewable natural polymer, and its active hydroxyl group can be easily modified to produce many kinds of derivatives.[6,7] By virtue of chemical stability, biocompatibility, biodegradability, and nontoxicity,[8] the cellulose and its derivatives as a chemical substance have been extensively used to develop the environment-friendly materials[9] and biomaterials.[10–13] Meanwhile, the microspheres, membranes,[10] and hydrogels[11] are the major forms of biomaterials, especially as the drug delivery systems[12] and tissue engineering scaffolds.[13] To further improve the performances of cellulose-based materials, blending with other biocompatible natural polymers has been applied as the simple and efficient method. For example, the carboxymethyl chitosan (CMC) was compounded into cellulose films to result in a good combination of antibacterial function and mechanical performances only by optimizing the CMC content[14] while the temperature-sensitive methyl cellulose was blended with pH-sensitive alginate to produce a new complex hydrogel with multi stimulus-response properties.[15]

Correspondence to: J. Huang (huangjin@iccas.ac.cn) or Y. Chen (yunchen@whu.edu.cn).

Contract grant sponsor: National Natural Science Foundation of China; contract grant number: 30570496.
Contract grant sponsor: State Key Laboratory of Pulp and Paper Engineering, South China University of Technology; contract grant number: 200514.
Contract grant sponsor: Key Laboratory of Cellulose and Lignocellulosics Chemistry, Guangzhou Institute of Chemistry, Chinese Academy of Sciences; contract grant number: LCLC-2005-172.

Soy protein isolate (SPI) is readily available from agricultural processing products,[16] and has been used to prepare biodegradable adhesives and plastics.[17] SPI can be thermoplastic processed with the aid of plasticizers to give many kinds of shaped products, which is expected to replace popular petroleum-based plastics. Furthermore, the nutritional and health benefits of soy protein[18] draw attention to the application in the field of biomedical materials,[19] such as tissue engineering scaffolds,[20] wound-dressing material,[21] and drug delivery system.[22] To further improve the function of soy protein-based biomaterials, other biocompatible polysaccharides, such as cellulose,[23,24] chitin,[25] and chitosan[26] were introduced. The predominant advantages of such blend materials possessed enhanced mechanical properties and inherited the bioactivities of soy protein and added polysaccharides.

In our previous work,[23,24] the SPI/cellulose blend membrane was prepared by solution casting, and now the biomedical application as tissue engineering scaffold has been ongoing. Herein, based on the thermoplasticity of SPI,[27] we attempt to develop the composites based on SPI and selected cellulose derivatives, such as methyl cellulose (MC), hydroxyethyl cellulose (HEC), and hydroxypropyl cellulose (HPC), by the thermoforming method. The resultant blends, which had the biodegradability and biocompatibility, were not only used as environmental-friendly materials, but as a potential biomedical material. The advantages of such SPI-based materials involved enhanced mechanical properties and the combined bioactivity of components. Moreover, the effects of side groups onto cellulose derivatives on the structure and mechanical properties were discussed.

EXPERIMENTAL

Materials

Commercial soy protein isolate (SPI) was purchased from DuPont-Yunmeng Protein Technology (Yunmeng, China). The weight-average molecular weight (M_w) of SPI was determined by multi-angle laser light scattering instrument (MALLS, DAWN® DSP, Wyatt Technology, USA) equipped with a He–Ne laser ($\lambda = 632.8$ nm) to be 2.05×10^5.[28] The original moisture content, protein content, and amino acid compositions of SPI have been investigated in our previous work, and the protein content of more than 90 wt % and the compositions of 18 diverse amino acids were summarized.[28] Three cellulose derivatives were supplied by Shandong Heda (Shandong, China), such as methyl cellulose (MC) containing $\sim$ 29.5 wt % methyl oxide groups, hydroxyethyl cellulose (HEC) with $\sim$ 1.9 of molar substituted degree, and hydroxypropyl cellulose (HPC) containing $\sim$63.0 wt % hydroxypropyl groups. Glycerol purchased from the Shanghai Chemical (Shanghai, China) was of analytical grade.

Preparation of blend sheets

A series of powders containing different cellulose derivatives (HEC, HPC, and MC) and SPI with desired weight ratios were mechanically mixed with the plasticizer of glycerol, respectively, and the weight ratio of every solid powder (including cellulose derivatives and SPI) and glycerol was controlled as 70 : 30 all the time. Subsequently, the glycerol-plasticized powders were compression-molded as the sheets at 140°C under the pressure of 20 MPa for 3 min, and then air-cooled to 50°C for half an hour before releasing the pressure for demolding. The dimension of the sheets with the thickness of $\sim$ 0.50 mm was about 70 mm $\times$ 70 mm. The resultant sheets were conditioned in a desiccator with silica gel as desiccant for 1 week at room temperature before characterization.

The resultant HPC/SPI, HEC/SPI, and MC/SPI blend sheets, were respectively, coded as HPC/SPI-*n*, HEC/SPI-*n*, and MC/SPI-*n*, where *n* represented the content of cellulose derivatives in the solid powder (n = 5, 10, 15, 20, 30, 40, and 50) before mixing with glycerol. At the same time, the sheet without cellulose derivatives was coded as SPI-S.

Characterization

X-ray diffraction (XRD) patterns were recorded on a D/max-2500 X-ray diffractometer (Rigaku Denki, Japan) with Cu Kα_1 radiation ($\lambda = 0.154$ nm) in a range of $2\theta = 3 \sim 50^\circ$ using a fixed time mode with a step interval of 0.02°. Additionally, the crystalline degree (χ_c) was calculated by the accessory software of instrument.

Differential scanning calorimetry (DSC) analysis was carried out on a DSC-204 instrument (Netzsch, Germany) under nitrogen atmosphere at a heating or cooling rate of 20°C/min. The sheets were scanned in the range of -150 to 100°C after a pretreatment (heating from 20 to 100°C and then cooling down to -150°C) of eliminating the thermal history.

Scanning electron microscope (SEM) observation was carried out on a X-650 scanning electron microscope (Hitachi, Japan). The sheets were frozen in liquid nitrogen and then snapped immediately. The fractured surfaces of the sheets were sputtered with gold and then observed and photographed.

The tensile strength (σ_b), elongation at break (ε_b), and Young's modulus (E) of the blend sheets were measured on a universal testing machine (CMT6503, Shenzhen SANS Test Machine, Shenzhen, China)

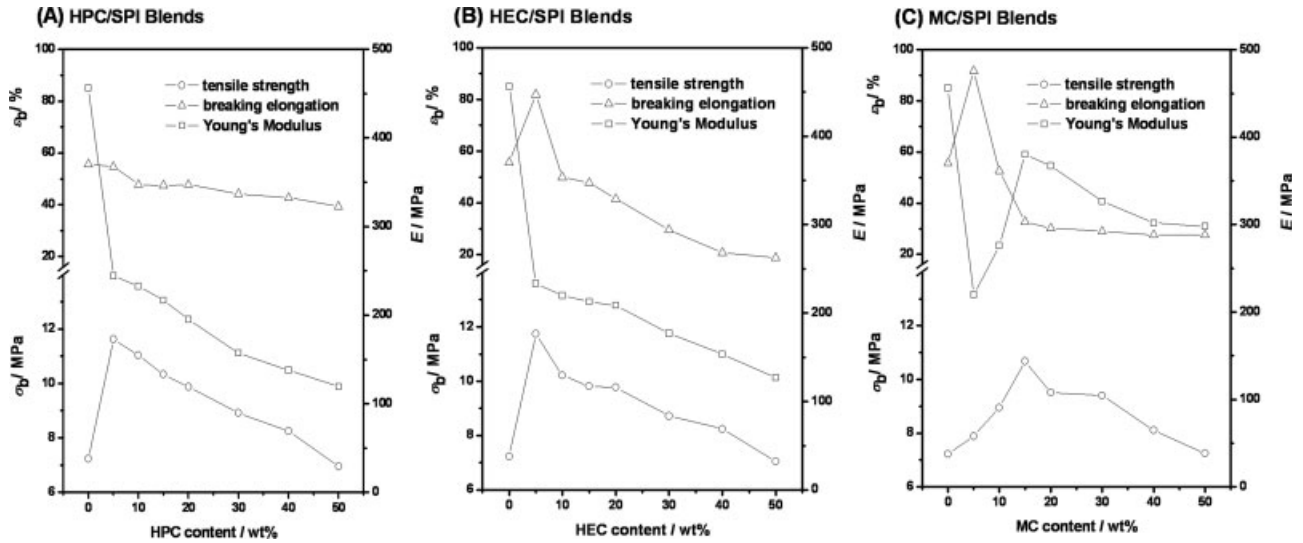

Figure 1 Effects of the cellulose derivative content on mechanical properties of the blend sheets based on SPI and various cellulose derivatives.

with a tensile rate of 5 mm/min according to GB13022-91. The tested samples were cut into the quadrate strips with the width of 10 mm, and the distance between testing marks was 40 mm. Before test, all the samples were conditioned under 35% relative humidity for 1 week. An average value of five replicates of each sample was taken.

RESULTS AND DISCUSSION

Mechanical performances of cellulose derivatives/SPI blends

Effects of the content and species of cellulose derivatives on the mechanical properties of the blend sheets are depicted in Figure 1, respectively. As shown in Figure 1(A), the tensile strength (σ_b) of the HPC/SPI sheets sharply increased up to the maximum value of 11.62 MPa from 7.23 MPa as adding 5 wt % HPC, and then gradually decreased with increasing HPC content from 10 to 50 wt %. Meanwhile, the Young's Modulus (E) and breaking elongation (ε_b) decreased with increasing HPC content, and especially the E of the HPC/SPI-5 containing 5 wt % HPC sharply decreased in contrast to the sharp increase of σ_b.

Figure 1(B) shows that the effects of HEC content on σ_b, ε_b, and E of the HEC/SPI blends were similar to those of the HPC content. However, compared with SPI-S, it was worth of noting that adding 5 wt % HEC resulted in a simultaneous enhancement in σ_b (from 7.23 to 11.74 MPa) and ε_b (from 55.64 to 81.92%), respectively.

As shown in Figure 1(C), the simultaneous enhancement in σ_b and ε_b also happened for the MC/SPI sheets containing 5 wt % MC, i.e., 7.89 MPa of σ_b and 91.8% of ε_b, as well as a sharp decrease of the E. Although the changes of ε_b functioned as the MC content for the MC/SPI blends showed a similar tendency to the those of the HPC/SPI and HEC/SPI blends, the effect of MC content on σ_b and E was obviously different, i.e., the σ_b and E firstly increased with increasing MC content and reached the maximum σ_b of 10.68 MPa and E when the MC content was 15 wt %, followed by a slight decrease as unceasingly increasing MC content.

Compared with the SPI-S sheet, the addition of cellulose derivatives resulted in the enhancement of strength when the content of cellulose derivatives was less than 40 wt %. Especially, the simultaneously increased ε_b was observed for the blend sheets containing 5 wt % HEC and MC. It might be attributed to the miscibility driven by the interaction between cellulose derivatives and SPI molecules as well as the structure of crystalline domains based on the aggregates of cellulose derivatives thereafter. Although the HPC with relatively hydrophobic chains did not represent the simultaneous enhancement of strength and elongation, the blend sheets filled by HPC can keep relatively high elongation when the HPC content is higher. It was pitiful that the E values of all blend sheets were lower than that of pure SPI-S sheet, resulting from the damage of original ordered structure in SPI matrix after introducing cellulose derivatives.

Structure and fractured morphology of HPC/SPI blends

Figure 2(A) shows the XRD patterns and crystalline degree (χ_c) of the HPC/SPI blend sheets with various HPC contents. The XRD pattern of SPI powder suggested that there existed some ordered structure, i.e., crystalline domains, shown as two peaks located at

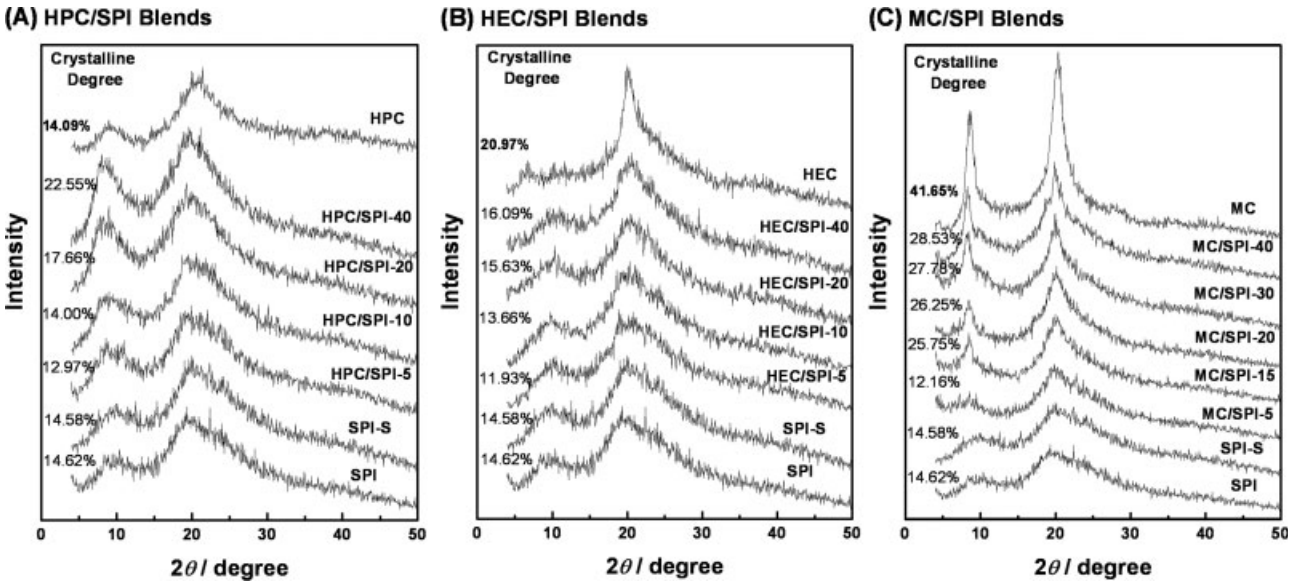

Figure 2 XRD patterns of the blend sheets based on SPI and various cellulose derivatives as well as SPI-S sheet and the powders of SPI and cellulose derivatives.

about 8.8 and 19.0° as well as the χ_c of 14.62%, which was inherited by the SPI-S sheet as well as a similar χ_c of 14.58%. In addition, the HPC powder was also semicrystalline, shown as two peaks at 9.0° and 21.0° as well as the χ_c of 14.09% in Figure 2(A). With an increase of HPC content, the peak at 9.0° gradually became prominent while the χ_c increased. When the HPC content was higher than 20 wt %, the χ_cs (17.66% and 22.55%) of the HPC/SPI sheets were higher than those of pure SPI-S sheet and HPC powder. However, the blend sheets containing the HPC content of < 10 wt % showed lower χ_cs in contrast to pure SPI-S sheet and HPC powder. Usually, the decrease of χ_c for the blends based on two semicrystalline components results from the good miscibility between components. As a result, a small amount of HPC (< 10 wt %) can interact with SPI at molecular level to produce a miscible blend. Thereafter, with increasing HPC content, the solubility limit of HPC in SPI matrix, i.e., the lack of miscibility, resulted in the increase of χ_c.

Figure 3 shows the effect of cellulose derivative content on glass transition temperature ($T_{g,onset}$) and

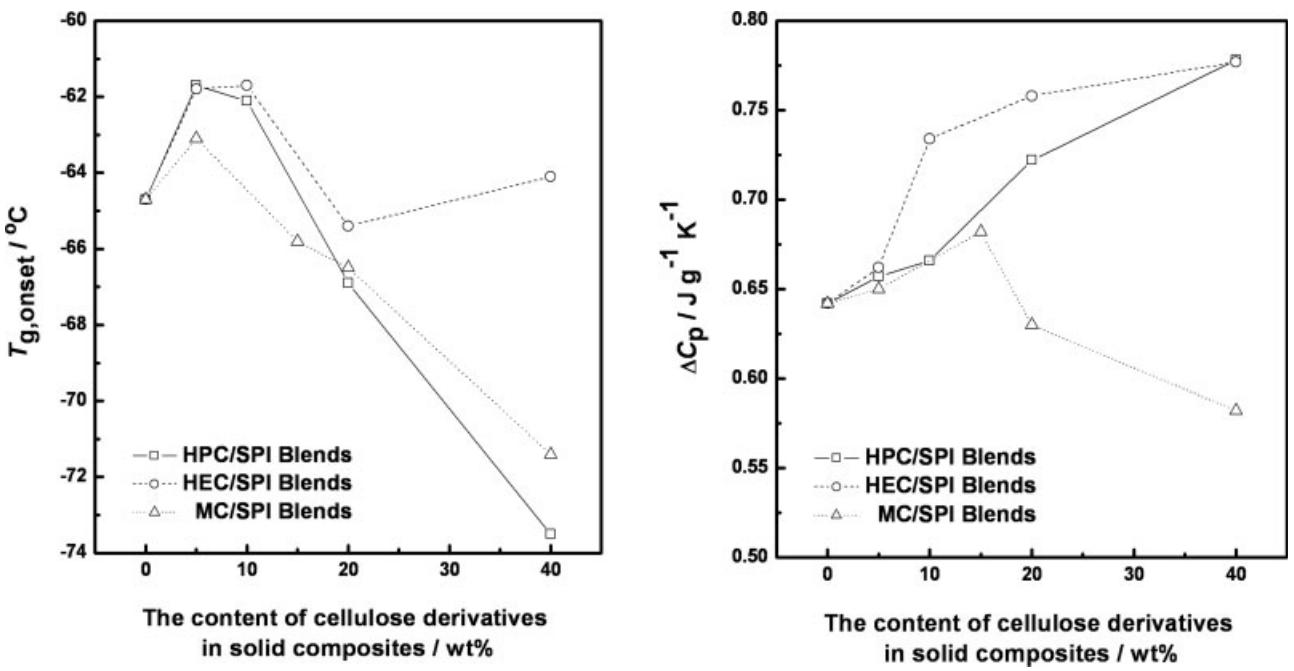

Figure 3 Effects of cellulose derivative content on glass transition temperature ($T_{g,onset}$) and heat-capacity increment (ΔC_p) for the blend sheets based on SPI and various cellulose derivatives.

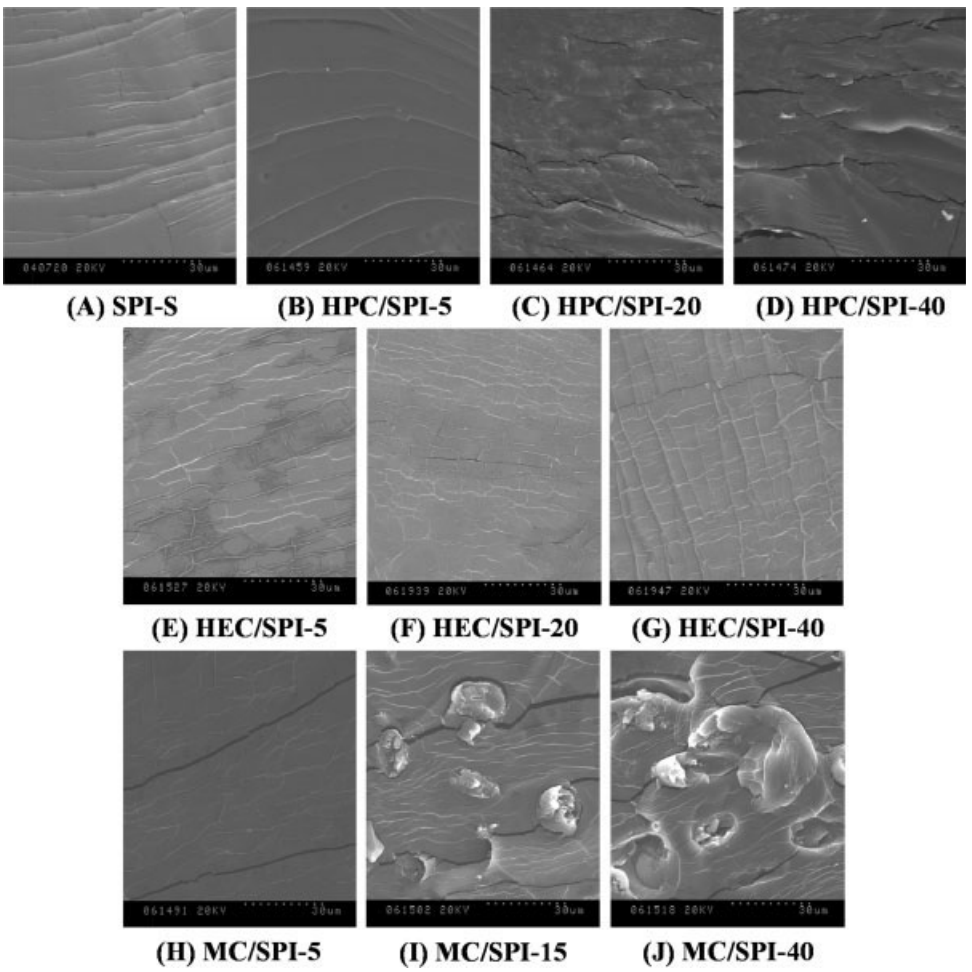

Figure 4 SEM images of fractured surface of blend sheets based on SPI and various cellulose derivatives as well as SPI-S sheet.

heat-capacity increment (ΔC_p) for three series of blends. The shifts of glass transition generally reflect the changes of chemical environments for one component in composites, which is associated with intermolecular interaction, spatial hindrance, microphase structure, and so on. Compared with the SPI-S sheet, the $T_{g,onset}$ firstly increased for HPC/SPI-5, and then gradually decreased with an unceasing increase of HPC content. The $T_{g,onset}$s of the HPC/SPI sheet containing < 10 wt % HPC were higher than that of the SPI-S sheet, indicating the motion of SPI chains was restricted. It resulted from the miscibility between HPC and SPI driven by the interaction at molecular level, which was in agreement with the XRD analysis. Thereafter, the solubility limit of HPC in SPI matrix produced two distinct domains assigned to the SPI and HPC components respectively. The weakened interaction between components as well as the increase of weight ratio of glycerol versus SPI, with increasing HPC content, resulted in the decrease of $T_{g,onset}$. On the other hand, the ΔC_p increased with increasing HPC content, indicating the restriction of HPC or its domain to SPI motion existed all the time.

Figure 4 shows the SEM images of fractured morphologies of the blend sheets based on SPI and various cellulose derivatives as well as SPI-S sheet. SPI-S showed a brittle fractured character with terrace morphology [Fig. 4(A)]. The XRD and DSC results suggested that a small amount of HPC was miscible with SPI and then the microphase separation occurred with an increase of HPC content. As a result, 5 wt % HPC immersed into SPI matrix to show a similar morphology of fractured surface [Fig. 4(B)] to SPI-S. Thereafter, many small pleats occurred in the fractured surface of HPC/SPI-20 sheet [Fig. 4(C)], which was assigned to the isolated HPC domains. As seen in the SEM images of HPC/SPI-40 with higher HPC content [Fig. 4(C)], the fractured surface became smoother because the scale of HPC domains extended and fused together to produce a homogeneous structure.

Structure and fractured morphology of HEC/SPI blends

Compared with HPC powder, the HEC powder showed more obvious crystalline character, seen as a dominant peak at 20.0° and higher χ_c (20.97%) in Figure 2(B). Different from the HPC/SPI blends, the XRD patterns of all the HEC/SPI blends in Figure 2(B) were similar to that of pure SPI-S sheet, and especially the intensity at 9.5° almost had no changes. In addition, the χ_c of all HEC/SPI blends were lower than that of HEC powder, suggesting that the crystalline structures of HEC powder might be partly destroyed in the thermoforming process. It was worth of noting that the χ_cs of the HEC/SPI sheets containing < 10 wt % HEC were even lower than pure SPI-S sheet, attributing to a certain extent of miscibility between the components. With an increase of HEC content, the χ_c of the HEC/SPI blends slightly increased, indicating that the HEC crystalline domains in the blends gradually formed and increased.

As seen in Figure 3, the effects of HEC content on $T_{g,onset}$ and ΔC_p were also similar to those of the HPC/SPI system except for a slight increase of the HEC/SPI-40's $T_{g,onset}$. The XRD analysis pointed out that semicrystalline HEC was miscible with SPI while the crystalline HEC domains formed and increased with increasing HEC content. As a result, compared with SPI-S sheet, higher $T_{g,onset}$ for the HEC/SPI blends containing < 10 wt % and higher ΔC_p for all the HEC/SPI blends also resulted from the restriction of HEC component to SPI motion. Thereafter, as the crystalline HEC structure increased, the $T_{g,onset}$ decreased because of the weaker restriction of crystalline domain than that of interaction at molecular level as well as an increase of weight ratio of glycerol versus SPI. However, with unceasingly increasing HEC content, overfull crystalline structures resulted in a slight increase for the HEC/SPI-40's $T_{g,onset}$.

Different from the fractured surface of the HPC/SPI sheets, the fractured surface of HEC/SPI sheets showed a network-like morphology, seen in Figure 4(E–G). The XRD and DSC analysis pointed out that the HEC aggregated as crystalline domains in the blends. As a result, the strips as network framework in the SEM images might be assigned to the crystalline HEC domains. With an increase of HEC content, the strips became more and more as well as the increase of strip scale and network density.

Structure and fractured morphology of MC/SPI blends

The MC powder had highest χ_c of 41.65% in three cellulose derivatives used in this work, and its XRD pattern in Figure 2(C) showed two sharp peaks located at 8.7° and 20.4°. Compared with SPI-S, the XRD patterns of the MC/SPI sheets also showed such two predominant peaks assigned to the crystalline character of MC except for the MC/SPI-5 sheet, suggesting that the MC had a stronger tendency of aggregating as isolated crystalline domains in SPI matrix. The similar pattern of MC/SPI-5 with lowest MC content to SPI-S as well as lower χ_c in contrast to SPI-S suggested the miscibility between MC and SPI. Thereafter, with an increase of MC content, the intensities of peaks assigned to MC crystalline for the MC/SPI sheets became stronger as well as an increase of χ_c that was higher than that of SPI-S, indicating that the isolated crystalline MC domains formed and increased with increasing MC content.

The strong aggregation of MC as isolated crystalline domain resulted in the different changes of $T_{g,onset}$ and ΔC_p functioned as MC content for the MC/SPI blends from those for the HPC/SPI and HEC/SPI blends. First, the $T_{g,onset}$ and ΔC_p of MC/SPI-5 increased and was higher than SPI-S sheet, resulting from the restriction of the MC component to SPI motion based on the interaction between MC and SPI, which was in agreement with the miscibility between components proved by XRD analysis. With an unceasing increase of MC content, MC self-aggregated as crystalline domains. At this time, the restriction to SPI motion gradually decreased, shown as a decrease of $T_{g,onset}$ that was even lower than that of SPI-S. Meanwhile, the decrease of ΔC_p lagged behind that of $T_{g,onset}$. The MC/SPI-15 with highest strength had a highest ΔC_p, suggesting that the crystalline MC domains can also be tightly associated with SPI matrix. Thereafter, the decrease of ΔC_p resulted from the decrease of effective contact area between MC domain and SPI matrix with the expansion of domain scale. Same as the HPC/SPI and HEC/SPI systems, the increase of weight ratio of glycerol versus SPI with increasing MC content was also the factor to decrease the $T_{g,onset}$ and ΔC_p.

The fractured surface of MC/SPI-5 with least MC in Figure 4(H) showed the similar network-like morphology to the HEC/SPI blends. However, the MC had a severer tendency of aggregation as crystalline domains. Consequently, with an increase of MC content, many MC domains located at the micrometer scale occurred on the fractured surface with dispersed strips, shown as Figure 4(I) of MC/SPI-15. Thereafter, the aggregated great domains became more and more as well as the increased domain scale, shown as Figure 4(J) of MC/SPI-40.

Structure–mechanical properties relationships

In the HPC/SPI blends, the HPC can interact with SPI at molecular level to produce a miscible blend as

the HPC content was lower than 10 wt %. At this time, the enhanced strength originated from the rigid main-chain of HPC as well as the intermolecular reaction between HPC and SPI. Subsequently, the isolated crystalline HPC domains formed and increased with an increase of HPC content, which inhibited the reinforcing function. Meanwhile, the damage of added HPC to the original ordered structure in SPI matrix resulted in the continual decrease of modulus and elongation. In addition, the entanglement and interaction between HPC and SPI restricted the decrease extent of ε_b and kept $\sim$ 40% when the HPC content was higher than $\sim$ 15 wt %, which was higher than other two systems.

The miscibility between SPI and 5 wt % HEC or 5 wt % MC, similar to the HPC/SPI blends, resulted in the simultaneous enhanced strength and elongation. However, the stronger aggregation of HEC and MC as crystalline domains in SPI matrix produced network-like morphology for the HEC/SPI blends and the MC/SPI blend containing 5 wt % MC as well as the domains of MC for the MC/SPI blend containing $>$ 15 wt %. The great scale and high density of crystalline network resulted in the decrease of strength and elongation for the HEC/SPI blends with an increase of HEC content. However, the moderate content of aggregated MC domain facilitated reinforcing materials. As a result, with increasing MC content, the strength and modulus firstly increased up to MC/SPI-15 and then decreased. Meanwhile, similar to the HPC/SPI blends, the lower modulus of the HEC/SPI and MC/SPI blends, in contrast to SPI-S, originated from the damage of original ordered structure in SPI as well.

Effects of side groups on the structure and mechanical properties of blends

The introduction of three cellulose derivatives with different side groups used in this work resulted in the formation of various structures in SPI matrix, such as the miscible blends containing low content of cellulose derivatives, the blends filled by network-like structure constructed with crystalline strips of cellulose derivatives and the blends with the dispersed domains. Obviously, the formations of these structures were closely associated with the difference of interaction and aggregated tendency caused by different side-group structure. The side chains of HPC and HEC were relatively longer and terminated with the hydroxyl group, which might interact with SPI matrix more facilely. In addition, compared with HEC, the HPC contained additional $-CH_3$ group in side chain and showed more hydrophobic. However, the MC has no longer side chain while active hydroxyl groups are also partly terminated with methyl groups. Consequently, it was certain that less association happened between MC and SPI matrix.

Because the long side chains of HPC and HEC can facilely interact with SPI molecules and even penetrated into SPI matrix to produce a structure of continuous phase, the miscible blends were produced as adding 10 wt % HEC or HPC in contrast to the limited 5 wt % of MC content. It was just as the relatively weak interaction between MC and SPI resulted in the stronger aggregated tendency and the formation of greater crystalline domains for MC. In addition, the hydrophilic HEC might be closely associated with SPI matrix more, and hence produces higher strength.

CONCLUSIONS

In this work, three cellulose derivatives, i.e., MC, HEC, and HPC, were introduced into soy protein thermoplastics to enhance mechanical performances. The effects of content and species of cellulose derivatives on mechanical properties mainly attributed to the miscibility between components as well as the structure and scale of interconnected network and great domain based on the crystalline aggregates of cellulose derivatives, which strongly depended on the structural character of side groups. When the content of cellulose derivatives was low (5 wt %), the miscibility between components improved the strength and even resulted in the simultaneous enhancement of strength and elongation for the HEC/SPI and MC/SPI blends. With unceasingly increasing the content of cellulose derivatives, the network of crystalline HEC and MC formed while the MC even aggregated as the great crystalline domains. Except that the moderate content of aggregated MC domains could also further enhance the strength, the reinforcing effect was inhibited on the whole.

Since the selected cellulose derivatives and soy protein are biodegradable and biocompatible, the resultant blends are not only the high-performance environment-friendly materials, but expected to apply in the field of biomedical materials, such as the tissue engineering scaffold.

References

1. Vogl, O.; Jaycoxm G. O. Prog Polym Sci 1999, 24, 3.
2. Puglia, D.; Tomassucci, A.; Kenny, J. M. Polym Adv Tech 2003, 14, 749.
3. Mecking, S. Angew Chem Int Ed 2004, 43, 1078.
4. Amass, W.; Amass, A.; Tighe, B. Polym Int 1998, 47, 89.
5. Chandra, R.; Rustgi, R. Prog Polym Sci 1998, 23, 1273.
6. Klemm, D.; Philipp, B.; Heinze, T.; Heinze, U.; Wagenknecht, W.; Comprehensive Cellulose Chemistry; WILEY-VCH Verlag GmbH: Weinheim, Germany, 1998.

7. Klemm, D.; Heublein, B.; Fink, H.-P.; Bohn, A. Angew Chem Int Ed 2005, 44, 3358.
8. Schurz, J. Prog Polym Sci 1999, 24, 481.
9. Nishino, T.; Matsuda, I.; Hirao, K. Macromolecules 2004, 37, 7683.
10. Tanaka, M.; Wong A. P.; Rehfeldt, F.; Tutus, M.; Kaufmann, S. J Am Chem Soc 2004, 126, 3257.
11. Chen, C.-H.; Tsai, C.-C.; Chen, W.; Mi, F.-L.; Liang, H.-F.; Chen, S.-C.; Sung, H.-W. Biomacromolecules 2006, 7, 736.
12. Uekama, K.; Matsubara, K.; Abe, K.; Horiuchi, Y.; Hirayama, F.; Suzuki, N. J Pharm Sci 1990, 79, 244.
13. Svensson, A.; Nicklasson, E.; Harrah, T.; Panilaitis, B.; Kaplan, D. L.; Brittberg, M.; Gatenholm, P. Biomaterials 2005, 26, 419.
14. Zhuang, X. P.; Liu, X. F. J Appl Polym Sci 2006, 102, 4601.
15. Liang H.-F.; Hong, M.-H.; Ho, R.-M.; Chung, C.-K.; Lin, Y.-H.; Chen, C.-H.; Sung, H.-W. Biomacromolecules 1917, 2004, 5.
16. Kaplan, D. L. Biopolymers from Renewable Resources; Springer-Verlag: Berlin, Heidelberg, 1998.
17. Kumar, R.; Choudhary, V.; Mishra, S.; Varma, I. K.; Mattiason, B. Ind Crop Prod 2002, 16, 155.
18. Friedman, M.; Brandon, D. L. J Agric Food Chem 2001, 49, 1069.
19. Zheng, H.; Zhou, Z.; Chen, Y.; Huang, J.; Xiong, F. J Appl Polym Sci 2007, 106, 1034.
20. Silva, G. A.; Vaz, C. M.; Coutinho, O. P.; Cunha, A. M.; Reis, R. L. J Mater Sci Mater Med 2003, 14, 1055.
21. Vaz, C. M.; de Graaf, L. A.; Reis, R. L.; Cunha, A. M. Mater Res Innovat 2004, 8, 149.
22. Vaz, C. M.; Van Doeveren, P. F. N. M.; Yilmaz, G.; De Graaf, L. A.; Reis, R. L.; Cunha, A. M. J Appl Polym Sci 2005, 97, 604.
23. Chen, Y.; Zhang, L.; J Appl Polym Sci 2004, 94, 748.
24. Chen, Y.; Zhang, L.; Liu, J.; Gu, J. J Membr Sci 2004, 241, 393.
25. Zheng, H.; Tan, Z.; Zhan, Y. R.; Huang, J. J Appl Polym Sci 2003, 90, 3676.
26. Silva, S. S.; Santos, M. I.; Coutinho, O. P.; Mano, J. F.; Reis, R. L. J Mater Sci Mater Med 2005, 16, 575.
27. Zhong, Z.; Sun, X. S. Polymer 2001, 42, 6961.
28. Wei, M.; Fan, L.; Huang, J.; Chen, Y. Macromol Mater Eng 2006, 291, 524.